Pemetrexed Improves Tumor Selectivity of ^{111}In-DTPA-Folate in Mice with Folate Receptor–Positive Ovarian Cancer

Cristina Müller[1], Roger Schibli[2,3], Eric P. Krenning[1], and Marion de Jong[1]

[1]Department of Nuclear Medicine, Erasmus Medical Center, Rotterdam, The Netherlands; [2]Center for Radiopharmaceutical Science, ETH-PSI-USZ, Paul Scherrer Institute, Villigen-PSI, Switzerland; and [3]Department of Chemistry and Applied Biosciences, ETH Zurich, Zurich, Switzerland

Folate-based radiopharmaceuticals can be used as imaging agents and for potential radiotherapy of folate receptor (FR)–positive malignant tissue (e.g., ovarian carcinomas). However, substantial FR expression in the kidneys results in undesired renal retention of radioactivity. Recently, we found that the preinjection of an antifolate significantly improved tumor selectivity of organometallic ^{99m}Tc-radiofolates in mice. The aim of this study was to corroborate the effect of pemetrexed with the clinically tested ^{111}In-DTPA-folate (DTPA is diethylenetriaminepentaacetic acid) in a human ovarian cancer xenografted mouse model. **Methods:** In vivo studies were performed in female athymic nude mice bearing subcutaneous FR-positive ovarian tumors (IGROV-1 and SKOV-3) or metastases (after intraperitoneal SKOV-3 cell inoculation). Biodistribution studies were performed 1, 4, and 24 h after administration of ^{111}In-DTPA-folate (0.7 MBq/mouse, 0.35 μg) with or without preinjection of pemetrexed (PMX, 400 μg) 1 h before the radiofolate. Images were acquired with a high-resolution, high-sensitivity SPECT/CT camera, 4 and 24 h after injection of the radiotracer (30–50 MBq/mouse, 4.5–10 μg). **Results:** In biodistribution studies the tumor uptake of ^{111}In-DTPA-folate (IGROV-1: 9.79 ± 3.21 %ID/g [percentage injected dose per gram]; SKOV-3: 7.57 ± 0.61 %ID/g, 4 h after injection) was high and retained over the time of investigation. However, considerable retention of radioactivity was found in kidneys (85–105 %ID/g, 4 h after injection), resulting in unfavorably low tumor-to-kidney ratios (~0.10). Preinjection of PMX resulted in a significant reduction of renal uptake (20%–30% of control values, $P < 0.03$) at all time points after injection of ^{111}In-DTPA-folate, whereas the tumor uptake was retained. Thus, the tumor-to-kidney ratio was significantly increased to ~0.50. SPECT/CT images confirmed the superior tumor-to-background ratio in mice injected with PMX. These findings were particularly evident in mice with SKOV-3 metastases that could be visualized only when ^{111}In-DTPA-folate was administered in combination with PMX. **Conclusion:** The application of PMX resulted in a significant reduction of undesired radioactivity accumulation in kidneys, whereas the tumor uptake remained unaffected. These observations suggest a general validity of the reducing effect of PMX on the uptake of radiofolates in kidneys. Our findings will lead the way toward the development of folate-based radiotherapy.

Key Words: folate receptor; ^{111}In-DTPA-folate; pemetrexed; SPECT/CT; SKOV-3

J Nucl Med 2008; 49:623–629
DOI: 10.2967/jnumed.107.047704

The development of tumor-selective radiopharmaceuticals is clinically desirable as a means of detecting or confirming the presence and location of primary and metastatic lesions and monitoring tumor response to (chemo)therapy. In addition, the application of targeted radiotherapeutics provides a unique and effective modality for direct tumor treatment.

Ovarian cancer is the leading cause of death among women with gynecologic malignancies, with an overall 5-y survival rate of <30% (American Cancer Society [www.cancer.org]). The survival rate has remained largely unchanged for many years due to the difficulties of an early diagnosis as well as the frequent resistance of these tumors to chemotherapy. Thus, there is a demand for reliable diagnostic modalities and alternative therapies. In this context, the high-affinity folate receptor (FR) emerged as a promising target because of its frequent overexpression in ovarian cancer (in >90% of the cases (*1,2*)) but limited expression in normal human tissues and organs. Folate conjugates of diverse radionuclides (^{99m}Tc (*3–8*), ^{111}In (*4,9*), $^{66/67/68}$Ga (*10,11*), and ^{18}F (*12*)) for SPECT or PET purposes have been developed and evaluated in (pre)clinical studies (*13,14*).

^{111}In-DTPA-folate (DTPA is diethylenetriaminepentaacetic acid) revealed favorable in vivo characteristics (*15*): high tumor uptake, efficient clearance from the blood, and an almost exclusive excretion via kidneys, which is particularly important because high-background radiation in the abdomen would interfere with imaging of ovarian carcinomas and metastases thereof. Kidneys were the only sites that accumulated unfavorably high radioactivity. These promising preclinical results

Received Sep. 27, 2007; revision accepted Dec. 6, 2007.
For correspondence or reprints contact: Cristina Müller, PhD, Department of Nuclear Medicine, Erasmus Medical Center, s-Gravendijkwal 230, 3015 CE Rotterdam, The Netherlands.
E-mail: cristina.mueller@psi.ch

achieved with ^{111}In-DTPA-folate led to Phase I and II clinical trials including 33 patients with either newly detected ovarian cancer or suspected recurrent ovarian or endometrial cancer (*9*). Although the sample size was too small to allow a final conclusion, the overall observations from this initial clinical study with ^{111}In-DTPA-folate were encouraging. The radiofolate appeared to be safe and effective for scintigraphic imaging to distinguish malignant from benign ovarian masses.

The high renal retention of radioactivity found in preclinical studies was confirmed in patients, indicating that the mouse is a useful model for predicting the tissue distribution of folate-based tracers in humans. Kidney uptake and retention is a common feature of any folate-based (radio)pharmaceutical due to FR expression on the luminal side of the brush border membrane in proximal tubule cells. FRs provide an efficient reabsorption mechanism for physiologic folates from primary urine, preventing the loss of these important vitamins (*16,17*). However, folate-based small-molecule radiopharmaceuticals encounter the same fate as physiologic folates after filtration in the renal glomeruli, resulting in significant radioactivity accumulation in the renal tissue.

Whereas high radioactivity accumulation in the kidneys can disturb imaging contrast of small metastases in the abdomen, it is in particular of concern with regard to a therapeutic application of radiofolates due to the risk of renal damage by particle-emitting radiation. In an attempt to face this issue, we recently developed a protocol that described the combined application of an organometallic ^{99m}Tc-radiofolate with antifolates (methotrexate, raltitrexed, pemetrexed [PMX]) in which PMX (*18*) appeared to be the most advantageous. Intravenous injection of PMX before the radiofolate resulted in a significant reduction of kidney accumulation of radioactivity without affecting the tumor uptake (*19,20*). This effect was reproducible with diverse organometallic ^{99m}Tc- or ^{188}Re-radiofolates previously developed by our group (*21*).

The aim of this study was to investigate whether the effect of PMX holds true also in combination with other than organometallic ^{99m}Tc-radiofolates. The general validity of our findings would allow further steps for the progression of therapeutic radiofolates. For this purpose we performed biodistribution and imaging studies with the clinically tested ^{111}In-DTPA-folate with and without preadministration of PMX. Our results are discussed with regard to future application of folate-based radiopharmaceuticals in nuclear medicine.

MATERIALS AND METHODS

Radiofolate Synthesis

The DTPA-folate ligand was a kind gift from Prof. Philip S. Low (Purdue University, West Lafayette, Indiana). The radiolabeling was performed according to the following procedure: a stock solution of DTPA-folate (10^{-3} mol/L) was mixed with phosphate-buffered saline (PBS), pH 6.5, and incubated with $^{111}InCl_3$ (Mallinckrodt-Tyco) with a specific activity of 2–7 MBq/μg DTPA-folate. The reaction mixture was incubated for 1–2 h at room temperature. Quality control was performed by high-performance liquid chromatography (HPLC) (Waters HPLC system, with a tunable absorbance detector; and a Unispec multichannel analyzer γ-detector, a Symmetry [Waters] C-18 reversed-phase column [5 μm, 25 cm × 4.6 mm] using an eluent that consisted of aqueous 0.05 M triethylammonium phosphate buffer, pH 2.25, and methanol with a linear gradient to 80% methanol over 30 min and a flow rate of 1.3 mL/min). The radiofolate was dissolved and administered to the animals in PBS, pH 6.5.

Cell Culture

IGROV-1 cells (human ovarian carcinoma) were a kind gift from Dr. Gerrit Jansen (Department of Rheumatology, Free University, Amsterdam, The Netherlands). SKOV-3 cells (human ovarian adenocarcinoma) were provided by Dr. Ilse Novak (Center for Radiopharmaceutical Science, Paul Scherrer Institute, Villigen, Switzerland). The cells were cultured as monolayers at 37°C in a humidified atmosphere containing 5% CO_2. Note that the cells were cultured in a folate-free cell culture medium, FFRPMI (modified RPMI, without folic acid, vitamin B_{12} and phenol red; Cell Culture Technologies GmbH). FFRPMI medium was supplemented with 10% heat-inactivated fetal calf serum ([FCS] as the only source of folate), L-glutamine, and antibiotics (penicillin/streptomycin/fungizone). Subconfluent cells were harvested by treatment with ethylenediaminetetraacetic acid (2.5 mmol/L) in PBS, pH 7.4. The cells were then washed once with PBS and pelleted by spinning at 1,000*g* for 5 min at 20°C. The cells were resuspended in PBS for subcutaneous inoculation (IGROV-1 and SKOV-3) or intraperitoneal injection (SKOV-3) of the mice.

Preparation of Mice Tumor Models

All animal experiments were approved by the governing Animal Welfare Committee and conducted in accordance with the regulations of the institution. Six to 8-wk-old female, athymic nude mice (NMRI *nu/nu*) were purchased from Charles River Laboratories. The animals were fed a folate-deficient rodent diet starting 5 d before the tumor cell inoculation (*22*). Mice were inoculated with the IGROV-1 or SKOV-3 cells respectively ($6–8 \times 10^6$ cells in 100 μL PBS) into the subcutis of each shoulder. In addition, another group of mice was injected intraperitoneally with SKOV-3 cells (7×10^6 cells in 400 μL PBS) to induce tumor metastases.

Biodistribution Studies

Radiofolate biodistribution studies were performed in triplicate, approximately 21 d after tumor cell inoculation, when the tumor reached a size of approximately 0.5–1.5 cm^3. For biodistribution studies, 0.7 MBq of ^{111}In-DTPA-folate (0.35 μg) in 100 μL PBS, pH 6.5, was administered via a lateral tail vein. PMX (LY231514; Eli Lilly) was diluted with 0.9% NaCl according to the instruction of the manufacturer. It was administered in the tail vein (400 μg in 100 μL), 1 h before the radiotracer. Blocking studies were performed with excess folic acid dissolved in PBS (100 μg in 100 μL) and administered instantaneously before the radiotracer. The animals were euthanized at 1, 4, or 24 h after administration of ^{111}In-DTPA-folate alone or with either preinjected PMX or coinjected folic acid. Selected tissues and organs were collected, weighed, and counted for radioactivity in a γ-counter (Wizard, 1480; Perkin Elmer). The results are presented as the percentage of the injected dose per gram

of tissue weight (%ID/g), using reference counts from a definite sample of the original injectate that was counted at the same time.

SPECT/CT

SPECT scans were performed with a 4-head multiplexing multipinhole camera (NanoSPECT/CT; Bioscan Inc.) (*23*). Each head was outfitted with a tungsten-based collimator with nine 1.4-mm-diameter pinholes providing a reconstructed resolution in the submillimeter range. The cylindric field of view (37 mm in diameter and 16 mm in length) could be extended using a step-and-shoot (SPECT) or continuous (CT) helical scan of the animal, with the user defining a range from 16 to 220 mm according to the region to be imaged. The acquisitions of mice bearing subcutaneous tumors (IGROV-1) were performed 4 or 24 h after injection of ^{111}In-DTPA-folate (30–50 MBq, 4.5–10 μg). The time per view was chosen as 120–150 s (IGROV-1 subcutaneous tumors) and as 450 s (SKOV-3 intraperitoneal metastases), resulting in a total scan duration of 40 min to 2 h. CT scans were performed with the integrated CT using a tube voltage of 45 kV and an exposure time of 1,500 ms per view. After acquisition, SPECT data were reconstructed iteratively with HiSPECT software (Scivis GmBH). For the CT reconstruction, a cone beam filtered backprojection was used. SPECT and CT data were automatically coregistered as both modalities shared the same axis of rotation. The fused datasets were analyzed using InVivoScope postprocessing software (Bioscan Inc.).

Ex Vivo Autoradiography

Autoradiography was performed with sections of tumors and kidneys from the mice that had been scanned 4 h after injection of ^{111}In-DTPA-folate (30 MBq, ~4.5 μg) with or without PMX or folic acid administration. Immediately after scanning, tumor tissue and kidneys were collected and frozen, embedded in TissueTek (O.C.T. Compound; Sakura Finetek Europe B.V.), and stored at −80°C. Frozen organs were cut into sections of 10 μm using a microtome (Cryo-Star HM 560 M) and mounted on slides (Superfrost plus; Menzel). The slides were exposed to phosphor imaging screens (type SR, 12.5 × 25.2 cm^2; Packard Instruments Co.) in x-ray cassettes overnight. The screens were then read by a phosphor imager (Cyclone; Packard Instruments Co.) to reveal the distribution of radioactivity in the sections.

Statistical Analysis

Statistical analyses were performed by using a *t* test (Microsoft Excel software). All analyses were 2-tailed and considered as type 3 (2-sample unequal variance). A P value < 0.05 was considered statistically significant.

TABLE 1
Biodistribution of ^{111}In-DTPA-Folate in IGROV-1 Tumor-Bearing Female Nude Mice

Biodistribution	1 h after injection	4 h after injection	24 h after injection
Blood	0.29 ± 0.01	0.21 ± 0.03	0.15 ± 0.02
Lung	1.81 ± 0.12	2.07 ± 0.33	1.43 ± 0.19
Spleen	0.82 ± 0.33	0.72 ± 0.27	0.68 ± 0.40
Kidneys	73.68 ± 16.23	85.61 ± 11.90	81.23 ± 6.34
Stomach	2.91 ± 0.03	3.21 ± 0.61	2.15 ± 0.40
Intestines	0.80 ± 0.09	1.43 ± 0.39	0.76 ± 0.12
Liver	9.97 ± 3.28	7.32 ± 1.08	4.41 ± 1.26
Muscle	1.65 ± 0.16	1.83 ± 0.06	1.35 ± 0.29
Bone	1.29 ± 0.08	1.51 ± 0.28	1.12 ± 0.32
Salivary glands	14.04 ± 3.03	12.18 ± 1.23	8.70 ± 1.56
Tumor	8.74 ± 0.89	9.79 ± 3.21	7.13 ± 2.37
Tumor-to-blood	29.55 ± 2.62	47.04 ± 12.59	49.96 ± 20.82
Tumor-to-liver	1.02 ± 0.33	1.34 ± 0.54	1.81 ± 0.98
Tumor-to-kidney	0.12 ± 0.02	0.11 ± 0.04	0.09 ± 0.03
	Pemetrexed*	Pemetrexed*	Pemetrexed*
Biodistribution	1 h after injection	4 h after injection	24 h after injection
Blood	0.29 ± 0.07	0.21 ± 0.11	0.09 ± 0.02
Lung	1.35 ± 0.13	1.33 ± 0.58	0.92 ± 0.36
Spleen	0.39 ± 0.05	0.47 ± 0.05	0.33 ± 0.14
Kidneys	21.59 ± 2.18	22.56 ± 1.95	19.43 ± 5.13
Stomach	2.31 ± 0.34	2.29 ± 0.73	1.40 ± 0.11
Intestines	0.39 ± 0.09	0.54 ± 0.22	0.51 ± 0.28
Liver	7.87 ± 0.93	4.44 ± 1.37	2.09 ± 0.26
Muscle	1.37 ± 0.51	1.25 ± 0.22	0.60 ± 0.10
Bone	0.74 ± 0.48	0.77 ± 0.12	0.49 ± 0.10
Salivary glands	8.47 ± 1.62	7.68 ± 0.79	4.11 ± 0.53
Tumor	8.13 ± 0.96	11.01 ± 1.76	7.87 ± 1.13
Tumor-to-blood	29.67 ± 9.41	61.61 ± 25.29	98.39 ± 9.60
Tumor-to-liver	1.05 ± 0.20	2.68 ± 1.00	3.71 ± 0.87
Tumor-to-kidney	0.38 ± 0.07	0.49 ± 0.09	0.45 ± 0.13

*400 μg, injected 1 h before injection of radiotracer.

RESULTS

Biodistribution Studies

We investigated the effect of PMX on the tumor uptake of ^{111}In-DTPA-folate and the retention of radioactivity in FR-positive kidneys and salivary glands and nontargeted tissues and organs in FR-positive tumor-bearing mice (Tables 1 and 2). The tumor uptake was high in both types of xenografts (IGROV-1: 9.79 ± 3.21 %ID/g; SKOV-3: 7.57 ± 0.61 %ID/g, 4 h after

TABLE 2
Biodistribution of ^{111}In-DTPA-Folate in SKOV-3 Tumor-Bearing Female Nude Mice

Biodistribution	4 h after injection	Pemetrexed* 4 h after injection
Blood	0.20 ± 0.04	0.14 ± 0.02
Lung	1.82 ± 0.07	1.31 ± 0.31
Spleen	0.69 ± 0.02	0.51 ± 0.13
Kidneys	103.38 ± 18.79	22.81 ± 4.69
Stomach	2.21 ± 0.29	1.60 ± 0.20
Intestines	0.72 ± 0.06	0.32 ± 0.07
Liver	3.98 ± 1.21	2.90 ± 1.18
Muscle	1.23 ± 0.13	0.96 ± 0.07
Bone	0.85 ± 0.15	0.57 ± 0.12
Salivary glands	12.12 ± 1.62	7.32 ± 1.25
Tumor	7.57 ± 0.61	10.82 ± 0.78
Tumor-to-blood	40.68 ± 4.14	79.99 ± 11.29
Tumor-to-liver	1.94 ± 0.68	4.12 ± 1.33
Tumor-to-kidney	0.08 ± 0.01	0.49 ± 0.10

*400 μg, injected 1 h before injection of radiotracer.

injection) and remained largely unaltered over 24 h, the time period of the investigation. Clearance from the blood-pool was fast and, consequently, radioactivity accumulation in nontargeted tissues and organs was negligible. However, significant radioactivity was found at all time points after injection in FR-positive kidneys (70–105 %ID/g) and salivary glands (7–14 %ID/g). The administration of PMX, 1 h before ^{111}In-DTPA-folate, resulted in a significant reduction of kidney accumulation of radioactivity (20–30 %ID/g of control values, $P < 0.03$), whereas the tumor uptake was not affected. The preinjection of PMX resulted in an even slightly increased accumulation of the ^{111}In-DTPA-folate in both tumor xenografts (IGROV-1: 11.01 ± 1.76 %ID/g and SKOV-3: 10.82 ± 0.78 %ID/g, 4 h after injection). However, these findings were significant only for SKOV-3 tumors ($P < 0.01$). The uptake in salivary glands that has previously proven to be FR-specific was somewhat lower (about 65% of controls) in mice that received PMX. In nontargeted tissues and organs, PMX injection did not alter the distribution pattern of radioactivity and led to % ID/g values that were largely comparable to control values. After coinjection of excess folic acid (100 μg) to block FRs, there was almost no radioactivity left in the tumor tissue (<0.6 %ID/g) (data not shown). However, in kidneys, we found 10%–15% of the radioactivity that was detected in the kidneys of control animals.

SPECT/CT

Imaging experiments were performed with a dedicated small-animal SPECT/CT camera.

Figure 1 shows images from IGROV-1 tumor-bearing female mice 4 h after injection of ^{111}In-DTPA-folate. A control mouse showed high radioactivity both in IGROV-1 tumor xenografts and in kidneys. Injection of excess folic acid resulted in an almost complete blockade of the tumor uptake, but residual (presumably FR-nonspecific) radioactivity was found in kidneys. Images of a mouse injected with PMX 1 h before the ^{111}In-DTPA-folate showed radioactivity uptake in the tumor comparable to that of the control mouse, but a significant reduction of radioactivity accumulation was found in the kidneys.

SPECT/CT scans of mice with intraperitoneal SKOV-3 metastases are shown in Figure 2. The images of a mouse with metastases and a mouse without metastases could barely be distinguished (Figs. 2A and 2B) because of the high accumulated radioactivity in the kidneys. However, distinct visualization of SKOV-3 metastases in the whole abdomen became accessible in an animal that was previously

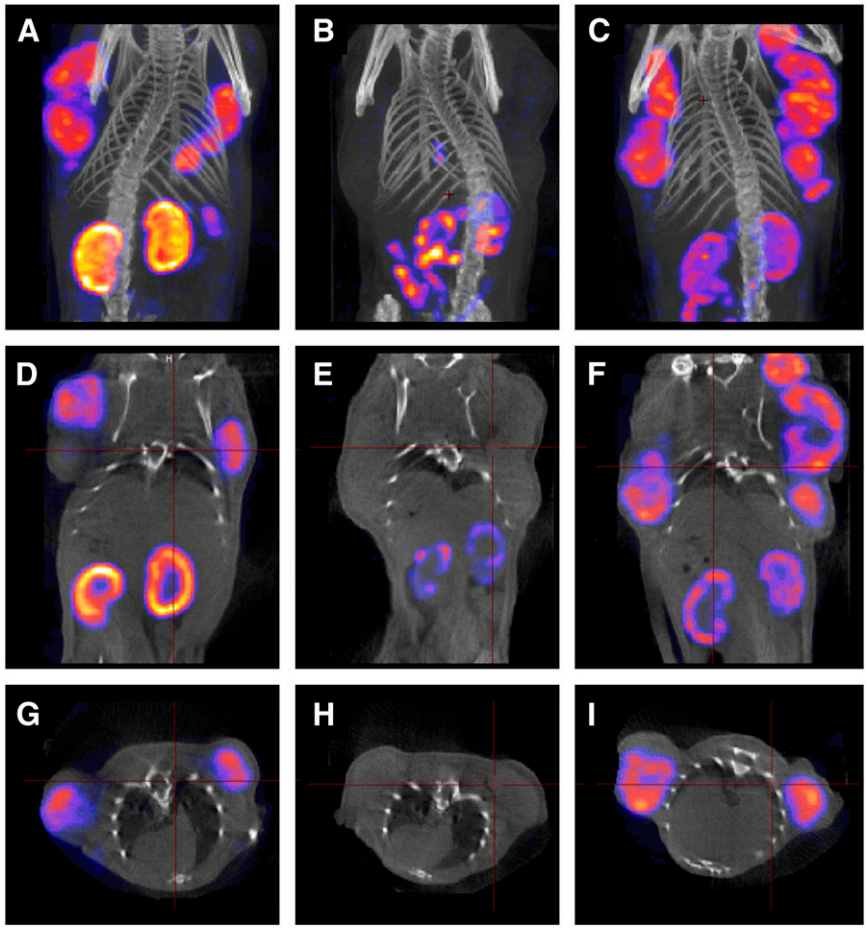

FIGURE 1. SPECT/CT images of female mice bearing subcutaneous IGROV-1 tumor xenografts, 4 h after injection of ^{111}In-DTPA-folate in a 3-dimensional view (A–C), as coronal (D–F) and transaxial sections (G–I). Control scan (A, D, and G), scan of a mouse coinjected with folic acid (B, E, and H), and scan of a mouse injected with PMX 1 h before injection of radiofolate (C, F, and I).

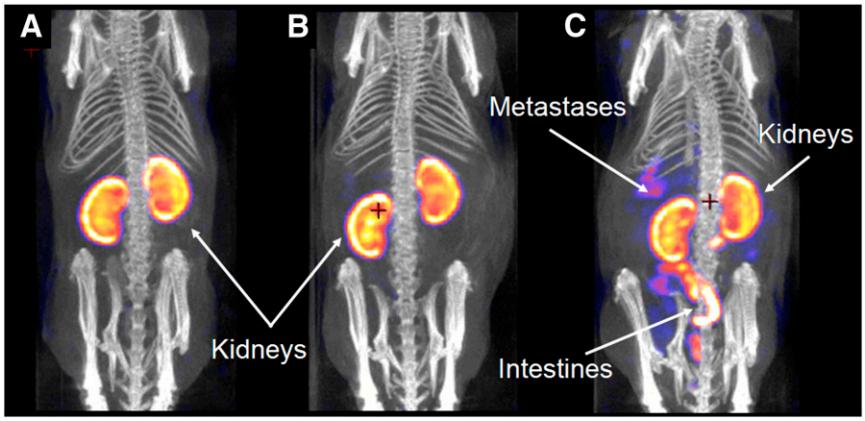

FIGURE 2. SPECT/CT images of female mice, 24 h after injection of ^{111}In-DTPA-folate. Images show a 3-dimensional view of a control mouse (without tumors; A) and mice with SKOV-3 intraperitoneal metastases that have been injected with radiofolate only (B) or with radiofolate in combination with PMX (C). Radioactivity scale was equalized to the same kidney uptake for all 3 mice.

injected with PMX as kidney uptake was reduced and the tumor-to-background contrast increased sufficiently (Fig. 2C).

Ex Vivo Autoradiography of Kidney Sections

Ex vivo autoradiography was performed with IGROV-1 tumors and kidneys of mice used for SPECT (Fig. 1), 4 h after injection of ^{111}In-DTPA-folate. Figure 3 shows IGROV-1 tumors from a control mouse, a mouse coinjected with folic acid, and a mouse preinjected with PMX. Whereas almost no radioactivity was found in tumors of the mouse that received folic acid, the tumors from the mouse injected with PMX could not be distinguished from control tumors. On the other hand, kidney sections of the mouse that received PMX and the mouse injected with folic acid showed a similar result—with significantly less radioactivity accumulation in the cortex, where FRs are expressed—compared with the autoradiograms of control kidney sections.

DISCUSSION

Recently, we discovered that the preinjection of PMX significantly decreased undesired kidney accumulation of radiofolates, whereas the tumor uptake was completely retained (*19*). PMX is an antifolate of the new generation with multiple enzyme targets that are involved in both pyrimidine and purine synthesis. PMX is approved by the Food and Drug Administration for the treatment of malignant mesothelioma in combination with cisplatin and as a single agent for the treatment of non–small cell lung cancer (*18*). Moreover, encouraging results were obtained in diverse clinical studies with PMX alone or in combination with other chemotherapeutics (e.g., gemcitabine) to treat a wide range of malignancies (e.g., carcinomas of the ovary, breast, colorectum, head and neck, uterine cervix, and so forth) (*18,24–27*). As structural analogs of folic acid, antifolates use the same transporters to gain entry into the cell interior. The FR that mediates cell internalization of folic acid and folate conjugates by endocytosis has been reported to bind PMX with an affinity similar to that of folic acid (*28*). However, the primary pathway of PMX to enter cells is the reduced folate carrier (RFC), a ubiquitously distributed bidirectional transporter and the major cellular transport system for physiologic (reduced) folates (*29*). In addition, a low-pH transporter has been described in the literature to be involved in PMX cell internalization (*30–33*). It was particularly unexpected that,

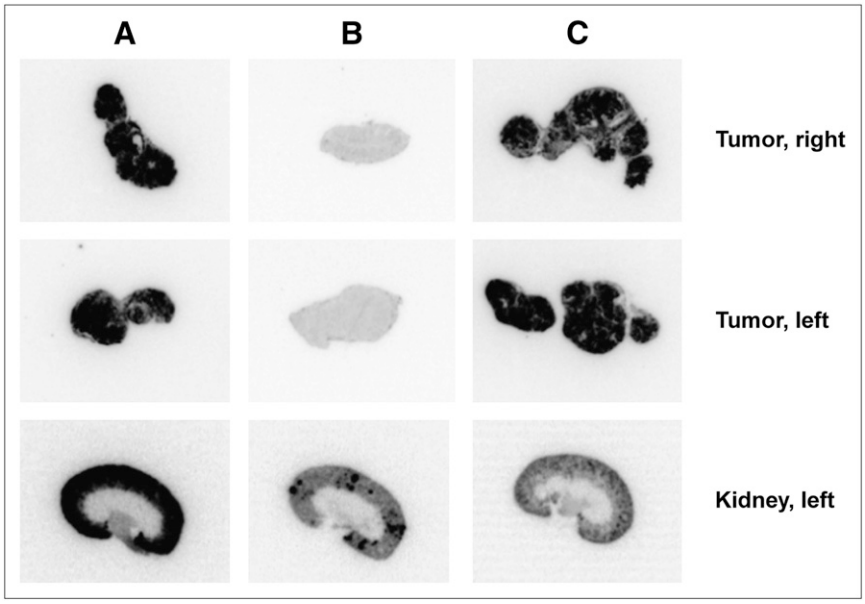

FIGURE 3. Ex vivo autoradiograms of IGROV-1 tumors and kidneys, 4 h after injection of ^{111}In-DTPA-folate (from mice shown in Fig. 1): control mouse (A), mouse that has been coinjected with folic acid (B), and mouse that received PMX 1 h before injection of radiofolate (C).

in contrast to folic acid or reduced folates, PMX did not influence the tumor uptake of radiofolates but blocked their uptake in the kidneys (*20*). We hypothesize that this is the result of an interplay of different uptake mechanisms for (radio)folates and PMX as well as different kinetics that might distinguish between (radio)folates and PMX, respectively. However, the exact mechanism of action of our observation is not yet elucidated.

In this study we tested PMX in combination with ^{111}In-DTPA-folate, the first radiofolate that had been advanced into clinical trials as an imaging agent of ovarian and endometrial cancer (*9*). Injection of the mice with PMX 1 h before ^{111}In-DTPA-folate showed a significantly improved tumor-to-background ratio of radioactivity as a result of an effective reduction of renal radioactivity accumulation. The time point for the preinjection of the antifolate was chosen according to our previous investigations (*19*) and was confirmed to be optimal to obtain the desired effect with ^{111}In-DTPA-folate as well. The data that have been acquired in biodistribution studies with mice bearing subcutaneous ovarian tumor xenografts were clearly confirmed by SPECT/CT and ex vivo autoradiography. Until now, it was not possible to visualize small SKOV-3 metastases in the abdomen of mice by SPECT/CT using FR-targeted radiopharmaceuticals. However, the administration of PMX to reduce kidney uptake and the high-resolution, high-sensitivity SPECT/CT camera (NanoSPECT/CT) used in this study allowed us to image SKOV-3 metastases in mice. These findings could be valuable for the detection of ovarian cancer and monitoring the effects of (chemo)therapy by noninvasive diagnostic imaging methods.

Our results suggest that PMX reduces kidney retention of any radiofolate, even though the extent of the blocking capacity is not equivalent for all folate conjugates. ^{111}In-DTPA-folate is known to be almost exclusively cleared via the kidneys; therefore, the kinetics differ significantly from those of organometallic ^{99m}Tc-radiofolates that showed high und undesired background radioactivity in the abdomen as a result of significant excretion via the gastrointestinal tract. Thus, it was not surprising that the blocking effect of PMX in kidneys was less pronounced for ^{111}In-DTPA-folate compared with the almost-complete kidney blockade found in combination with organometallic ^{99m}Tc-radiofolates. In vivo experiments performed with mice that received ^{111}In-DTPA-folate coinjected with excess folic acid resulted in an entire tumor blockade, as it was the case for other radiofolates. However, in the kidneys we still found retention of radioactivity (~10 %ID/g, 4 h after injection). These observations suggest that the residual radioactivity in the kidneys after administration of PMX or folic acid can be ascribed to the fraction that was nonspecifically accumulated due to renal excretion, which offers the possibility of reducing it with conventional methods such as amino acid infusion (*34,35*).

It is noteworthy that the methods used in this study—biodistribution, SPECT/CT, and autoradiography—were performed under slightly different conditions with regard to the amount of radioactivity and the folate mass injected. SPECT experiments required significantly higher amounts of radioactivity than necessary for biodistribution studies to obtain images of high quality that could be acquired within a reasonable time frame. Consequently, data of the biodistribution studies, SPECT/CT, and autoradiography can be compared only qualitatively. By any means, the translation of our findings to the human situation must be investigated carefully in patients with regard to the dosage and the ratio of the radiofolate and antifolate.

Epithelial ovarian cancer usually presents as advanced disease when therapy is rarely curative. After radical surgery that is followed by standard platinum- and taxane-based chemotherapy, there is no effective treatment for relapsed or metastatic disease (*36,37*). Therefore, direct tumor treatment with radiotherapeutics would provide a unique and effective modality. Targeting the FR is particularly intriguing, as it is overexpressed in 90% of serous ovarian cancers (but not in normal ovarian epithelium) and its expression increases in concentration with tumor progression and grade (*2,38*). However, to date, FRs in the kidneys that were at the same time targeted by folate conjugates remained an unsurmountable hurdle for the development of folate-based radiotherapy. A 10-fold higher uptake in kidneys compared with the tumor accumulation would certainly lead to renal damage by particle-emitting radiation. We believe that the application of PMX provides an opportunity to initiate folate-based radiotherapy. However, it has to be critically acknowledged that using PMX solely as a substance for kidney protection of radiation injury is problematic because PMX is a chemotherapeutic drug that can cause side effects (*18,24*). On the other hand, there is preclinical evidence of radiosensitization of tumor cells by PMX (*39,40*), which would be advantageous for folate-based radiotherapy. Preclinical in vitro and in vivo studies are ongoing to investigate the potential of this combination for therapy. The proof of an additive or synergistic effect of PMX and a therapeutic radiofolate would favor the translation of this combination into the clinics.

CONCLUSION

On the basis of the present and previous preclinical studies, we conclude that the combination of any radiofolate with PMX can prevent high and undesired radioactivity retention in kidneys while tumor accumulation of radioactivity is completely maintained. Consequently, the application of therapeutic radiofolates can be taken into consideration when applied in combination with PMX. This would be particularly interesting if the preinjection with PMX showed a synergistic effect on tumor cell treatment.

ACKNOWLEDGMENTS

We thank Prof. Philip S. Low for providing the DTPA-folate. We thank Dr. Christian Lackas and Dr. Nils Schramm for support with the NanoSPECT/CT.

REFERENCES

1. Garin-Chesa P, Campbell I, Saigo PE, Lewis JL, Old LJ, Rettig WJ. Trophoblast and ovarian cancer antigen LK26: sensitivity and specificity in immunopathology and molecular identification as a folate-binding protein. *Am J Pathol.* 1993;142:557–567.
2. Toffoli G, Cernigoi C, Russo A, Gallo A, Bagnoli M, Boiocchi M. Overexpression of folate binding protein in ovarian cancers. *Int J Cancer.* 1997; 74:193–198.
3. Guo WJ, Hinkle GH, Lee RJ. ^{99m}Tc-HYNIC-folate: a novel receptor-based targeted radiopharmaceutical for tumor imaging. *J Nucl Med.* 1999;40:1563–1569.
4. Mathias CJ, Hubers D, Low PS, Green MA. Synthesis of [^{99m}Tc]DTPA-folate and its evaluation as a folate-receptor-targeted radiopharmaceutical. *Bioconjug Chem.* 2000;11:253–257.
5. Leamon CP, Parker MA, Vlahov IR, et al. Synthesis and biological evaluation of EC20: a new folate-derived, ^{99m}Tc-based radiopharmaceutical. *Bioconjug Chem.* 2002;13:1200–1210.
6. Reddy JA, Xu LC, Parker N, Vetzel M, Leamon CP. Preclinical evaluation of ^{99m}Tc-EC20 for imaging folate receptor-positive tumors. *J Nucl Med.* 2004; 45:857–866.
7. Müller C, Hohn A, Schubiger PA, Schibli R. Preclinical evaluation of novel organometallic ^{99m}Tc-folate and ^{99m}Tc-pteroate radiotracers for folate receptor-positive tumour targeting. *Eur J Nucl Med Mol Imaging.* 2006;33:1007–1016.
8. Müller C, Schubiger PA, Schibli R. Synthesis and in vitro/in vivo evaluation of novel ^{99m}Tc(CO)$_3$-folates. *Bioconjug Chem.* 2006;17:797–806.
9. Siegel BA, Dehdashti F, Mutch DG, et al. Evaluation of ^{111}In-DTPA-folate as a receptor-targeted diagnostic agent for ovarian cancer: initial clinical results. *J Nucl Med.* 2003;44:700–707.
10. Mathias CJ, Wang S, Low PS, Waters DJ, Green MA. Receptor-mediated targeting of ^{67}Ga-deferoxamine-folate to folate-receptor-positive human KB tumor xenografts. *Nucl Med Biol.* 1999;26:23–25.
11. Mathias CJ, Lewis MR, Reichert DE, et al. Preparation of ^{66}Ga- and ^{68}Ga-labeled Ga(III)-deferoxamine-folate as potential folate-receptor-targeted PET radiopharmaceuticals. *Nucl Med Biol.* 2003;30:725–731.
12. Bettio A, Honer M, Müller C, et al. Synthesis and preclinical evaluation of a folic acid derivative labeled with ^{18}F for PET imaging of folate receptor-positive tumors. *J Nucl Med.* 2006;47:1153–1160.
13. Ke CY, Mathias CJ, Green MA. The folate receptor as a molecular target for tumor-selective radionuclide delivery. *Nucl Med Biol.* 2003;30:811–817.
14. Ke CY, Mathias CJ, Green MA. Folate-receptor-targeted radionuclide imaging agents. *Adv Drug Deliv Rev.* 2004;56:1143–1160.
15. Mathias CJ, Wang S, Waters DJ, Turek JJ, Low PS, Green MA. Indium-111-DTPA-folate as a potential folate-receptor-targeted radiopharmaceutical. *J Nucl Med.* 1998;39:1579–1585.
16. Goresky CA, Watanabe H, Johns DG. Renal excretion of folic acid. *J Clin Invest.* 1963;42:1841–1849.
17. Birn H, Spiegelstein O, Christensen EI, Finnell RH. Renal tubular reabsorption of folate mediated by folate binding protein 1. *J Am Soc Nephrol.* 2005;16:608–615.
18. Paz-Ares L, Bezares S, Tabernero JM, Castellanos D, Cortes-Funes H. Review of a promising new agent: pemetrexed disodium. *Cancer.* 2003;97:2056–2063.
19. Müller C, Brühlmeier M, Schubiger AP. Schibli R. Effects of antifolate drugs on the cellular uptake of radiofolates in vitro and in vivo. *J Nucl Med.* 2006;47: 2057–2064.
20. Müller C, Schibli R, Forrer F, Krenning EP, de Jong M. Dose-dependent effects of (anti)folate preinjection on ^{99m}Tc-radiofolate uptake in tumors and kidneys. *Nucl Med Biol.* 2007;34:603–608.
21. Müller C, Schubiger PA, Schibli R. Isostructural folate conjugates radiolabeled with the matched pair ^{99m}Tc/^{188}Re: a potential strategy for diagnosis and therapy of folate receptor-positive tumors. *Nucl Med Biol.* 2007;34:595–601.
22. Mathias CJ, Wang S, Lee RJ, Waters DJ, Low PS, Green MA. Tumor-selective radiopharmaceutical targeting via receptor-mediated endocytosis of gallium-67-deferoxamine-folate. *J Nucl Med.* 1996;37:1003–1008.
23. Forrer F, Valkema R, Bernard B, et al. In vivo radionuclide uptake quantification using a multi-pinhole SPECT system to predict renal function in small animals. *Eur J Nucl Med Mol Imaging.* 2006;33:1214–1217.
24. Rollins KD, Lindley C. Pemetrexed: a multitargeted antifolate. *Clin Ther.* 2005;27:1343–1382.
25. Misset JL, Gamelin E, Campone M, et al. Phase I and pharmacokinetic study of the multitargeted antifolate pemetrexed in combination with oxaliplatin in patients with advanced solid tumors. *Ann Oncol.* 2004;15:1123–1129.
26. Kalykaki A, Vamvakas L, Agelaki S, et al. A dose escalation study of gemcitabine plus pemetrexed administered biweekly in patients with solid tumors. *Oncology.* 2006;71:197–203.
27. Hensley ML, Derosa F, Gerst SR, et al. A phase I study of pemetrexed (P) plus gemcitabine (G) in relapsed ovarian cancer (OC): dosing results and evidence of activity. *J Clin Oncol.* 2006;24:276S–276S.
28. Theti DS, Jackman AL. The role of α-folate receptor-mediated transport in the antitumor activity of antifolate drugs. *Clin Cancer Res.* 2004;10:1080–1089.
29. Zhao RB, Babani S, Gao F, Liu LB, Goldman ID. The mechanism of transport of the multitargeted antifolate (MTA) and its cross-resistance pattern in cells with markedly impaired transport of methotrexate. *Clin Cancer Res.* 2000;6:3687–3695.
30. Wang YH, Zhao RB, Chattopadhyay S, Goldman ID. A novel folate transport activity in human mesothelioma cell lines with high affinity and specificity for the new-generation antifolate, pemetrexed. *Cancer Res.* 2002;62:6434–6437.
31. Wang YH, Zhao RB, Goldman ID. Characterization of a folate transporter in HeLa cells with a low pH optimum and high affinity for pemetrexed distinct from the reduced folate carrier. *Clin Cancer Res.* 2004;10:6256–6264.
32. Sierra EE, Goldman ID. Characterization of folate transport mediated by a low pH route in mouse L1210 leukemia cells with defective reduced folate carrier function. *Biochem Pharmacol.* 1998;55:1505–1512.
33. Zhao RB, Hanscom M, Chattopadhyay S, Goldman ID. Selective preservation of pemetrexed pharmacological activity in HeLa cells lacking the reduced folate carrier: association with the presence of a secondary transport pathway. *Cancer Res.* 2004;64:3313–3319.
34. Bernard BF, Krenning EP, Breeman WA, et al. D-Lysine reduction of indium-111 octreotide and yttrium-90 octreotide renal uptake. *J Nucl Med.* 1997;38:1929–1933.
35. Barone R, Pauwels S, De Camps J, et al. Metabolic effects of amino acid solutions infused for renal protection during therapy with radiolabelled somatostatin analogues. *Nephrol Dial Transplant.* 2004;19:2275–2281.
36. Kuhn WC. Therapy for recurrent ovarian cancer. *Curr Womens Health Rep.* 2003;3:33–38.
37. Tummala MK, McGuire WP. Recurrent ovarian cancer. *Clin Adv Hematol Oncol.* 2005;3:723–736.
38. Kelemen LE. The role of folate receptor alpha in cancer development, progression and treatment: cause, consequence or innocent bystander? *Int J Cancer.* 2006;119:243–250.
39. Bischof M, Weber KJ, Blatter J, Wannenmacher M, Latz D. Interaction of pemetrexed disodium (ALIMTA, multitargeted antifolate) and irradiation in vitro. *Int J Radiat Oncol Biol Phys.* 2002;52:1381–1388.
40. Mauceri HJ, Seetharam S, Salloum RM, Vokes EE, Weichselbaum RR. Treatment of head and neck and esophageal xenografts employing Alimta and concurrent ionizing radiation. *Int J Oncol.* 2001;19:833–835.